

# CLUSTER CORRELATION IN MIXED MODELS

A. Gardini, S.A. Bonometto

Dipartimento di Fisica G. Occhialini – Università di Milano–Bicocca

INFN sezione di Milano – Via Celoria 16, I20133 Milano, ITALY

e-mails: gardini@mi.infn.it – bonometto@mi.infn.it

G. Murante

Osservatorio Astronomico di Torino – Pino Torinese

e-mail: giuseppe@to.astro.it

G. Yepes

Departamento de Física Teórica C–XI – Universidad Autónoma de Madrid

Cantoblanco – 28049 Madrid, SPAIN

e-mail: gustavo.yepes@uam.es

Received \_\_\_\_\_; accepted \_\_\_\_\_

## ABSTRACT

We evaluate the dependence of the cluster correlation length  $r_c$  on the mean intercluster separation  $D_c$ , for three models with critical matter density, vanishing vacuum energy ( $\Lambda = 0$ ) and COBE normalized: a tilted CDM (tCDM) model ( $n = 0.8$ ) and two blue mixed models with two light massive neutrinos yielding  $\Omega_h = 0.26$  and  $0.14$  (MDM1 and MDM2, respectively). All models approach the observational value of  $\sigma_8$  (and, henceforth, the observed cluster abundance) and are consistent with the observed abundance of Damped Lyman $\alpha$  systems. Mixed models have a motivation in recent results of neutrino physics; they also agree with the observed value of the ratio  $\sigma_8/\sigma_{25}$ , yielding the spectral slope parameter  $\Gamma$ , and nicely fit LCRS reconstructed spectra.

We use parallel AP3M simulations, performed in a wide box (side  $360 h^{-1}\text{Mpc}$ ) and with high mass and distance resolution, enabling us to build artificial samples of clusters, whose total number and mass range allow to cover the same  $D_c$  interval inspected through APM and Abell cluster clustering data.

We find that the tCDM model performs substantially better than  $n = 1$  critical density CDM models. Our main finding, however, is that mixed models provide a surprisingly good fit of cluster clustering data.

PACS: 95.35; 98.80; 98.65.Cw

*Subject headings:* dark matter: massive neutrinos, large scale structure of the universe, methods: numerical, galaxies: clustering, clusters

## 1. Introduction

The study of the clustering of galaxy clusters, in the early eighties, allowed a basic advancement in our understanding of Large Scale Structure (LSS). The discrepancy between the galaxy correlation length  $r_g$  and the cluster correlation length  $r_c$  (Bahcall & Soneira 1983, Klypin & Kopylov 1983, but see also Hauser & Peebles 1973) led to the introduction of the concept of bias (Kaiser 1984). Data on  $r_c$  were then worked out, in further detail, for Abell clusters by Peacock & West (1992) and Postman, Huchra & Geller (1992), as well as for clusters in APM and in Edinburgh–Durham Southern Galaxy catalogs, by Dalton et al (1992), Nichol et al (1992) and Croft et al (1997).

These analyses show that the value of  $r_c$  depends on the mass threshold ( $M_{th}$ ) of the cluster sample, through its mean intercluster separation  $D_c = n^{-1/3}( > M_{th})$ , and that  $r_c$  increases with  $D_c$ . However,  $r_c$  values obtained from Abell and APM data seem only partially consistent; this is to be partially ascribed to different cluster definitions; Bahcall & Burgett (1986), Bahcall & Cen (1992) and Bahcall & West (1992) suggested that observational ambiguities are wide enough to allow to conjecture that the scaling relation  $r_c \simeq 0.4 D_c$  holds for  $20 < D_c h/\text{Mpc} < 100$ . Herebelow, we shall refer to this relation as BW conjecture. It ought to be born in mind that, above  $\sim 50 h^{-1}\text{Mpc}$ , such conjecture hinges on the estimates of  $r_c$  for 55 and  $94 h^{-1}\text{Mpc}$  mean separations, for richness  $R \geq 1$  and  $R \geq 2$  Abell clusters, while APM data, for the same  $D_c$  range, give smaller  $r_c$ . Dekel et al (1989) and Sutherland & Efstathiou (1991) suggested that the projection effects and peculiar inhomogeneities in the Abell sample might have biased upward  $r_c$  at large  $D_c$ . Peacock & West (1992), instead, confirmed such points (see also Jing, Plionis & Valdarnini, 1992). Altogether, it may be fair to say that the controversy on the observational behaviour of  $r_c$  for high  $D_c$  values has not been solved yet, although, as we shall see, there may be good reasons to assess that different cluster definitions play a key role.

This paper is devoted to a comparison of cluster clustering, as it emerges from such data, with simulations of three cosmological models: a tilted CDM (tCDM) model and two mixed models (MDM1 and MDM2) with cold+hot DM. All models have critical matter density, vanishing vacuum energy, and are COBE normalized. During the last few years, much attention has been devoted to models with a positive cosmological constant  $\Lambda$ , also because of the remarkable data sets concerning SN Ia (see, e.g., Riess et al 1998, Perlmutter et al 1998, and references therein). In this work, we shall not debate whether mixed models can still offer a fair fit to all cosmological data; they certainly do not fit SN Ia data, unless their current interpretation was misled by some systematic bias. In a number of cases, however, mixed models were just not tested and the success of  $\Lambda$ -models to fit some data set was directly taken as further evidence in their favour. In the case of cluster clustering, we shall show that mixed models perform quite well and are surely better than any other model with matter density parameter  $\Omega_m = 1$  considered until now.

In order to fit cluster data with a model, a large simulation volume is required; in fact, we need a fair sample of galaxy clusters for large  $D_c$ , as well as adequate mass and force resolutions, to identify clusters in a reliable way, for small  $D_c$ . Simulation parameters are therefore set so to allow a sample of 90 clusters, at least, for large  $D_c$  and  $\sim 60$  baryon-CDM particles per cluster, at least, for small  $D_c$  (as we shall see, 60 particles correspond to  $\sim 10^{14} h^{-1} M_\odot$ ). Altogether, at redshift  $z = 0$ , we shall therefore span a  $D_c$  interval ranging from  $\sim 20$  to  $80 h^{-1} \text{Mpc}$ .

Cluster clustering has been studied by various authors in simulations. In particular, the behaviour of  $r_c$  vs.  $D_c$ , for standard CDM and open CDM, was studied by Bahcall & Cen (1992), Watanabe et al (1994), Croft & Efstathiou (1994), Eke et al (1996), Croft et al (1997), Governato et al (1999). Their results allow to conclude that CDM models with  $n = 1$  may approach the observed behaviour of  $r_c$  vs.  $D_c$ , only for  $\Omega_m < 1$ . The behaviour

of  $r_c$  vs.  $D_c$  in a mixed model was also studied, using PM simulations, by Klypin & Rhee (1994) and Walter and Klypin (1996). Their work treated a different mix from those considered here, using smaller box and resolution. Accordingly, they could inspect only the  $D_c$  interval running from  $\sim 20$  to  $45 h^{-1}\text{Mpc}$ . The behaviour they found is only marginally consistent with a constant  $r_c/D_c$  ratio, but their model does not exhibit much improvement in respect to pure CDM.

The mixed models we consider here were selected on the basis of recent tests on  $\nu$  flavour mixing, which seem to support a non-vanishing  $\nu$ -mass. Mixing data come from the solar  $\nu$  deficit (see, e.g., Hampel et al 1996, for GALLEX, and Abdurashitov et al 1996, for SAGE), the atmospheric  $\nu$  anomaly (Fukuda et al 1994) and the LSND experiment (Athanasopoulos et al 1995) on  $\nu$ 's arising from  $\mu^+$  and  $\pi^+$  decay. Barger, Weiler & Whisnant (1998) and Sarkar (1999) show that all above results can agree if a fourth sterile  $\nu$  exists, which can be however added without harming BBNS or LEP standard results. Diagonalizing the mass matrix, they eventually obtain the four  $\nu$ -mass eigenvalues, which split into two nearly degenerate pairs, corresponding to  $m_\nu \simeq 0$  and  $m_\nu \sim 1.4\text{--}1.5$  eV. It must be outlined that, within this picture, there remains no contradiction among different experimental results, at variance with earlier analyses which seemed to find contradictions between LSND and other  $\nu$ -mixing results.

In a cosmological context, however, mixed models have been considered since long. The transfer function for several mixed models was first computed by Bonometto & Valdarnini (1984). Results on mixed models were then found by a number of authors (see, e.g., Achilli, Occhionero & Scaramella 1985, Valdarnini & Bonometto 1985, Holtzmann 1989, for results obtainable from the linear theory, and Davis et al 1992, Klypin et al 1993, Ghigna et al 1994, for early simulations). After the release of LSND data, Primack et al (1995) performed simulations of models with 2 massive  $\nu$ 's and yielding  $\Omega_h = 0.20$  and

found that such mixture eased some problems met by greater  $\Omega_h$  models. The possibility of considering mixed models together with blue spectra (primeval spectral index  $n > 1$ ) was first considered by Liddle et al (1996) and Lucchin et al (1996). In the former paper, blue mixed models able to fit all linear and analytical constraints were shown to exist. In the latter paper, inflationary models leading to blue spectra were discussed and results of an N-body simulation of blue mixed models were reported. Unfortunately, the model considered violated some observational constraints. A systematic study of blue mixed models was recently performed by Bonometto & Pierpaoli (1998) and Pierpaoli & Bonometto (1999), selecting those consistent with CMB data and data predictable from the linear theory.

In the next section we show that the models considered here, on the basis of  $\nu$ -physics motivation, are also suitable to fulfill the main observational constraints. In § 3 we review the technique used to simulate their non-linear evolution. In § 4 we describe how clusters are selected in simulations. Then, in § 5 we describe how the 2-point correlation function and its error estimates were worked out. In § 6, we will show the main results of the  $r_c$  vs.  $D_c$  behaviour derived from fits to the 2-point functions. § 7 is devoted to discussion of the results and the main conclusions we derived from this work.

## 2. Model parameters

The mixed models discussed in this paper were already considered in a previous work by Gardini, Bonometto & Murante (1999; hereafter Paper I) They are models with two equal-mass massive  $\nu$ 's, selected by requiring agreement with data which can be fitted using the linear theory. More in detail, we required, first of all, agreement with observations at top and bottom scales, i.e. with COBE data and with the observed Damped Lyman $\alpha$  system (DLAS) abundance (Storrie-Lombardi et al. 1995). Assuming 2 massive  $\nu$ 's

with  $m_\nu \geq 1.5 \text{ eV}$ , we adjusted the spectral index  $n$  so to agree with the above top and bottom data, choosing the minimum allowed value for the spectral amplitude ( $A_\Psi$ ). Over intermediate scales, the main constraints to be tested are at 8 and 25  $h^{-1}\text{Mpc}$ , where we evaluated the mass variances  $\sigma_{8,25}$  (see below). From such values we can work out the expected spectral slope and cluster abundance (again, see below); comparing their values with observations we see that  $m_\nu$  values up to  $\sim 3 \text{ eV}$  can be considered, without violating such constraints. Accordingly, we considered two values for the hot–dark–matter (HDM) density parameter  $\Omega_h$ , yielding  $m_\nu$  at the top and bottom of the allowed interval.

A CDM model, selected so to fit the same data in a similar way, was also studied, for the sake of comparison. While mixed models require  $n > 1$ , even with low  $A_\Psi$ , CDM may fit COBE data only if  $n < 1$ .

Model parameters are shown in detail in Table I, while fig. 1 shows the spectra obtained from the linear transfer function  $T(k)$  against APM reconstructed spectral points (Baugh & Gatzagaña 1996). The wavenumber  $k$  is related to the comoving length scale  $L = 2\pi/k$  and to the mass scale  $M = (4\pi/3)\rho_o L^3$ , where  $\rho_o$  is the present density of the Universe. In Fig. 1 also other data and results are shown, which will be discussed below.

EDITOR: PLACE TABLE 1 HERE.

The tCDM model approximates the APM galaxy spectrum slightly better than the standard CDM (sCDM), thanks to its increased slope. However, it lays still quite below the spectral points around the peak at  $k \simeq 5 \times 10^{-2} h \text{ Mpc}^{-1}$  (comoving length  $\lambda \simeq 100\text{--}120 h^{-1}\text{Mpc}$ ). Blue mixed models, instead, show a stronger spectral peak, occurring where  $\nu$  free streaming bends a primeval spectrum steeper than Zel’dovich. This causes a steeper downward spectrum for  $5 h^{-1}\text{Mpc} \lesssim \lambda \lesssim 50 h^{-1}\text{Mpc}$ , which might be related to the reasons why blue mixed models approach the  $r_c$  vs.  $D_c$  behaviour up to large  $D_c$ .

EDITOR: PLACE FIGURE 1 HERE.

Mass variances are defined according to the relation

$$\sigma^2(L) = \frac{\pi}{9} \left(\frac{x_o}{L}\right)^{n+3} A_\Psi \int_0^\infty du u^{n+2} T^2 \left(\frac{u}{L}\right) W^2(u) , \quad (1.1)$$

with a top-hat window function  $W(u) = 3(\sin u - u \cos u)/u^2$  and

$$P(k) = \frac{2\pi^3}{3} \frac{A_\Psi}{x_o^3} (x_o k)^n . \quad (1.2)$$

Here  $x_o$  is the comoving horizon distance. Using eq. (1.1) we estimate the parameter

$$\Gamma = 7.13 \times 10^{-3} (\sigma_8/\sigma_{25})^{10/3} , \quad (1.3)$$

which, only for pure CDM models, is often approximated as  $\Gamma \simeq \Omega_o h$  (see Efstathiou et al (1992). Peacock & Dodds (1994), using APM data, and Borgani et al. (1994) using Abell/ACO samples, constrained  $\Gamma$  within the  $(2\sigma)$  intervals 0.19–0.27 and 0.18–0.25 respectively. This parameter therefore tests the spectral slope above cluster mass scales.

Values of  $\sigma_8$  are directly related to the expected cluster number densities. A direct fit of data with simulations, for the cluster mass function, is given in Paper I, where, however, a different definition of cluster mass was used. This point will be discussed again below and will be deepened in a forthcoming work.

### 3. The simulations

The three simulations considered here were already used in Paper I, to which we refer for details. They were performed using a parallel N-body code, based upon the serial public AP3M code of Couchman (1991), extended in order to treat variable mass particle sets and used varying the time-steps, when needed. We considered a box of side  $L = 360 h^{-1}\text{Mpc}$



( $h$  is the Hubble parameters in units of  $100 \text{ km s}^{-1} \text{ Mpc}^{-1}$ ); here CDM+baryons were represented by  $180^3$  particles, whose individual mass is  $m_{180} = 2.22 \times 10^{12} h^{-1} M_{\odot}$  for  $\Lambda$ CDM. Mixed models also involve 2 massive  $\nu$ 's with  $m_{\nu} \simeq 3.02 \text{ eV}$  and  $1.63 \text{ eV}$ , to yield  $\Omega_h = 0.26$  and  $0.14$  (MDM1 and MDM2, respectively). Hence, *slow* particles, representing CDM+baryons, have masses  $\Omega_s m_{180}$  with  $\Omega_s = \Omega_{CDM} + \Omega_{bar} = 0.74$  and  $0.86$ , respectively, while *fast* particles, representing HDM, have masses  $\frac{1}{2}\Omega_h m_{180}$  (the ratio 2:1 between fast and slow particle numbers is required to set initial conditions with locally vanishing linear momentum). Our force resolution can be reported to a Plummer–equivalent smoothing parameter  $\epsilon_{pl} \simeq 40.6 h^{-1} \text{ kpc}$ . The comoving force and mass resolutions approach the limits of the computational resources of the machine we used (an HP Exemplar SPP2000 X Class processor of the CILEA consortium at Segrate–Milan). The numerical resolution of our simulations were similar to other simulations of pure CDM, with different initial conditions performed by Colberg et al. (1997), Thomas et al. (1997), Cole et al. (1997), and Governato et al (1999). Mixed model simulations with a comparable dynamical range, instead, have only been performed by Gross et al. (1998), but in a smaller volume.

#### 4. Cluster selection

Different criteria can be used to select clusters in simulations. In paper I, we identified clusters as virialized haloes. Here we shall give results obtained with a cluster definition aimed to approach more closely their observational definition. However, we widely tested and compared results ensuing different definitions, and a comprehensive discussion of the fit between particle sets obtained with various criteria will be published elsewhere. Let us however state that 2–point function outputs are fairly robust; although specific values of the clustering length  $r_c$ , at various  $D_c$ , have even significant variations, when the cluster definition is changed, the general trend is always preserved: the mixed models discussed

here however fit observational data. We shall illustrate this point with a few examples, without giving outputs for whole sets of different cluster definitions.

In order to approach the observational pattern, here clusters were found with a spherical overdensity (SO) algorithm, based on a fixed sphere radius  $R_a = 1.5 h^{-1}\text{Mpc}$ . The details of the procedure are close to those suggested by Croft & Efstathiou (1994) and Klypin & Rhee (1994). Hence, effects arising from the limiting magnitude of (observational) samples, border effects and projection effects are not included. (Also the sphere radius is fixed to mimic the Abell cluster definition; clusters found in the APM survey were selected also with smaller  $R_a$ . Our simulations were also used to test whether systematic effects arise from a different choice of  $R_a$ ; the differences we found have no significant impact on the results that will be shown here.)

More in detail, we start the procedure with a FoF algorithm, which finds sets of  $N$  CDM–baryon particles closer than  $f$  times the average inter–particle separation. Results reported here are obtained using  $f = 0.2$  and  $N = 25$ . Centers–of–mass (CM) of FoF groups are then inspected as possible centers for SO. Starting from them, we follow an iterative procedure: CDM–baryon particles within a distance  $R_a$  from CM and their CM are found; this is repeated until we reach a stable particle set and fix their CM. Only particle sets containing at least 25 particles are however kept. When, during the iterative procedure, two spheres intersect, only the most massive particle set is kept. Our procedure aims to find *all* clusters above a suitable mass scale. Loose requirements were therefore set on  $f$ , in order to explore any possible matter condensation; the dependence of our results on  $N$  was also tested. Reducing  $N$  obviously leads to more FoF groups and a number of them survives the iteration procedure defined hereabove. Most of such *extra–clusters*, however, do not contain many particles. The result of such tests can be summarized by stating that *extra–clusters* of more than  $\sim 60$  particles, found lowering  $N$  down to 12, are less than

$\sim 0.3\%$ , in all cases; this percentage has no further increase when still lower  $N$  are taken. Henceforth, for  $N > 60$ , i.e., for  $M > 1.3\Omega_s 10^{14} h^{-1} M_\odot \equiv M_{min}$ , our cluster samples can be considered complete. In fig. 2, we show the relation between cluster masses and  $D_c$  values, both at  $z = 0$  and at  $z = 0.8$ .

EDITOR: PLACE FIGURE 2 HERE.

Among other tests, we also verified the size of virialized haloes contained in clusters, as a function of their mass  $M_c$ . Let  $R_v$  be the radius encompassing a sphere, whereinside the density contrast is 180, found starting from the CM of each cluster, but whose actual center is attained through a suitable number of iterations, so to be the CM of all particles within  $R_v$  from it. Let then  $M_v$  be the mass of all CDM+baryon particles within  $R_v$ . For large clusters,  $R_v$  may exceed  $R_a$ ; when  $M_c$  is approximately  $< 7\Omega_s \cdot 10^{14} h^{-1} M_\odot$ , in general it is  $M_v < M_c$ . In fig. 3 we show the values of  $M_v$ , as a function of  $M_c$ , for  $\Lambda$ CDM. The trend is quite similar for mixed models.

EDITOR: PLACE FIGURE 3 HERE.

Although  $M_v$  tends to increase with  $M_c$ , the trend is clearly not monotonic; this is due to the spread of the values we find for  $R_v$  at any  $M_c$ . In spite of that, for  $M > M_{min}$ , all clusters contain a virialized halo. However, if we order by mass the cluster set, using  $M_v$  instead of  $M_c$ , we find a different result. Hence, cluster sets, whose mean distance is  $D_c$ , are different if we use  $M_v$  instead of  $M_c$ . It is then significant to compare the dependence of  $r_c$  on  $D_c$  for the two different orderings. In Paper I, clusters were given  $M_v$  as mass; such definition is farther from observational criteria, but is likely to be closer to physical requirements, e.g., if we aim to compare simulation outputs with the expectations of a Press & Schechter approach. Herebelow, in a few cases, we shall test how the clustering length

depends on  $D_c$ , when  $M_v$  replaces  $M_c$ . As we shall see, outputs depend significantly on the model, but are substantially independent from the cluster definition.

## 5. Cluster 2–point correlation function

Using clusters in our simulation box, ordered according to their  $M_c$ , we computed the 2–point correlation function  $\xi(r)$ , for a set of  $D_c$  values, by applying the estimator

$$\xi(r) = \frac{D_c^6 N_{pairs}(r)}{L^3 \delta V(r)} - 1 . \quad (3.1)$$

Here  $N_{pairs}(r)$  is the number of cluster pairs in the radial bin of volume  $\delta V(r)$ , centered on  $r$ , and  $L^3$  is the box volume. Error bars for  $\xi(r)$  were estimated using the standard bootstrapping procedure. (We checked the convergence of the estimator of the standard deviation evaluated from bootstrap realizations, by inspecting the third moment of the bootstrap distribution. In all cases, convergence was attained when the number of bootstrap realizations matched the number of points in the catalogues; see e.g. Bradley 1982) We compared such errors with the usual Poisson errors, which were found to be systematically smaller by a factor  $\sim 2$ .

We then performed two different fits to a power law

$$\xi(r) = (r/r_c)^{-\gamma} , \quad (3.2)$$

over the distance range  $5 h^{-1}\text{Mpc} < r < 25 h^{-1}\text{Mpc}$ : (i) A *constrained* fit, assuming a constant  $\gamma = 1.8$ . For the sake of example, in fig. 4 we show such fit for  $D_c = 30 h^{-1}\text{Mpc}$ .

EDITOR: PLACE FIGURE 4 HERE.

(ii) An *unconstrained* fit, allowing both  $r_c$  and  $\gamma$  to vary. Points were weighted by the corresponding bootstrap errors and  $r_c$  best–fit values are also given with bootstrap

errors. Such errors are obviously smaller for the constrained fit, where our ignorance on  $\gamma$  is hidden. In general, large  $D_c$  clusters yield best fit  $\gamma$  values approaching 2, although 1.8 lays always within  $1\sigma$ . Our  $r_c$  estimates are performed at  $z = 0$  and  $z = 0.8$ , to inspect cluster clustering evolution.

## 6. Results

In fig. 5 we report the  $r_c$  vs.  $D_c$  behaviour for tCDM, MDM1 and MDM2, for fixed  $\gamma = 1.8$ . In fig. 6 we give results for the same cases, obtained with 2–parameters fits on  $r_c$  and  $\gamma$ . Errors bars represent  $1\sigma$  bootstrap errors (see § 3). Of course, error bars are smaller in the single parameter fits, where our ignorance on  $\gamma$  is hidden.

Together with the  $r_c$  values obtained from our simulations we also plot APM and Abell cluster data, the BW conjecture, and the results from simulations performed by Bahcall & Cen (1992) and Croft & Efstathiou (1994). Recent results obtained by Governato et al (1999), for a critical CDM model, lay between the last two curves. Observational points and error bars given in our figures were obtained from original work. We draw the reader’s attention on the fact that, in some recent work studying cluster clustering in simulations, observational points and error bars are not accurately reported.

EDITOR: PLACE FIGURE 5 HERE.

EDITOR: PLACE FIGURE 6 HERE.

A comparison of tCDM with data, shows that simulated and APM data points are in fair agreement. In view of the better fits obtainable with mixed models, shown in the same figures, one might tend to overlook the improvement of tCDM in respect to CDM

models with  $n = 1$ , which, instead, is significant. Our  $\Lambda$ CDM model, however, seems to miss systematically the Abell catalog points and, thence, is far from the BW conjecture, which tries to set a compromise between Abell and APM results.

From this point of view, the performance of mixed models is better. For low  $D_c$ , MDM1 tends to give  $r_c$  values above the BW conjecture (see, however, Lee & Park 1999). A similar, but less pronounced, effect exists also for MDM2. On intermediate scales MDM1 sticks on the BW conjecture curve and meets two of the APM points at the  $2\text{-}\sigma$  level only. MDM2, instead, seems to try to compromise between APM and Abell points. On top scales, the behaviours shown here by the two models are opposite. The MDM1 behaviour, at such scales, seems however somehow anomalous; such scales are those which are most likely affected by cosmic variance and the MDM1 behaviour at  $D_c > 65\text{--}70 h^{-1}\text{Mpc}$  should certainly be tested with different model realizations. Furthermore, unconstrained fits tend to indicate that such discrepancy arises from different correlation function slopes.

It may also be significant to consider the unconstrained fit obtained ordering clusters according to  $M_v$  masses, which is shown in fig. 7. Let us notice that: (i) in most cases, error bars are smaller; (ii) the peculiar feature for MDM1 at large  $D_c$  has disappeared. It is likely that such improvement is related to a more direct physical significance of the mass  $M_v$  and the (variable) radius  $R_v$ . Taking a fixed radius  $R_a$ , instead, risks to accentuate a dependence on local peculiar features. In principle, this is more likely to occur for small mass clusters, for which significant volumes, still unaffected by virialization processes, lay within  $R_a$ . In our simulation volume, however, we have a large deal of low-mass clusters and this allows an efficient averaging over local realizations. At the top mass end, instead, the sample is more restricted and we must mostly rely on the virialization process, rather than on sample averaging, to smear off local peculiarities. Our results seem to indicate that significant memory of initial conditions is kept also below  $R_v$ .

EDITOR: PLACE FIGURE 7 HERE.

In Fig.s 8 and 9 we report a comparison between the 2–point function results at  $z = 0$  and  $z = 0.8$ , obtained using  $M_c$ .

EDITOR: PLACE FIGURE 8 HERE.

EDITOR: PLACE FIGURE 9 HERE.

Unconstrained fits at  $z = 0.8$  are rather noisy at large  $D_c$ , in particular for top scales. Constrained fits, instead, might be taken as an indication of clustering evolution on top scales. Here, perhaps, there is a further evidence of anomaly in MDM1, which is the only case when clustering seems however weaker at  $z = 0$  than at  $z = 0.8$ . Apparently, all models seem to indicate a greater clustering length at scales between 50 and  $65\text{--}70 h^{-1}\text{Mpc}$  for  $z = 0.8$ . Apart of MDM1, instead, this is inverted above  $70 h^{-1}\text{Mpc}$ .

EDITOR: PLACE FIGURE 10 HERE.

Fig 10, instead, shows results on cluster evolution based on  $M_v$  ordering and using constrained fits. The kind of evolution found hereabove seems confirmed, while MDM1 anomaly is reduced.

## 7. Discussion

Previous numerical results on cluster clustering, based on models with  $\Omega_m = 1$ , gave a behaviour of  $r_c$  vs.  $D_c$  a few  $\sigma$ 's below observational results. The only exception are Bahcall

& Cen (1992), whose numerical study involves peculiar extrapolations and however succeeds to meet two APM points at large  $D_c$  only. When considering subcritical CDM models (OCDM), the same authors obtain a behaviour close to the BW conjecture. However, this is not fully confirmed by later numerical studies; although they clearly indicate that, in OCDM models, the  $D_c$  dependence on  $r_c$  is consistent with APM points, Abell cluster points seem to require a still steeper dependence than in OCDM. Such findings, however, were currently interpreted as an indication that observational data on cluster clustering may be approached only by models with  $\Omega_m < 1$  and led to arguing that the observed dependence of  $r_c$  on  $M_{th}$  is somehow related to an early cluster formation.

The behaviour we find for tCDM does not support such kind of inference. Taking a spectral index  $n \neq 1$  has no substantial effect on the time of cluster formation, which is quite similar to standard CDM. In view of the more striking outputs for mixed models, we must not disregard the result we find for tCDM. The  $r_c$  vs.  $D_c$  behaviour of clusters in such model is analogous to previous outputs for OCDM and lays well above the very behaviour obtained by Bahcall & Cen (1992) for standard CDM. Our findings are that, taking  $n < 1$ , the clustering of clusters in an  $\Omega_m = 1$  model approaches the behaviour obtained from APM cluster data.

Even more striking is the cluster clustering behaviour for the mixed models considered in this work, which are based on low mass  $\nu$ 's. In this case, the slope of the  $r_c$  vs.  $D_c$  behaviour approaches the BW conjecture and, more significantly, within 1 or 2- $\sigma$  bootstrap error bars, we mostly find consistency both with APM and Abell results. The only exception could be the point of Abell clusters of richness  $R > 2$ , which is approached only by MDM2. Our results, however, support previous claims that, at the top mass end, wider samples may be required to suppress the cosmic variance.

Quite in general, it can be reasonable to consider cluster clustering as a measure of



the spectral power on scales exceeding  $\sim 25 h^{-1}\text{Mpc}$ . All models with  $\Omega_m = 1$  ought to have similar values of  $\sigma_8$ , in order to be consistent with the observed cluster abundance. Accordingly, the power at scales  $\sim 25 h^{-1}\text{Mpc}$  is basically gauged by the value of the  $\Gamma$  parameter. It may not be a case that models perform in a better way as their  $\Gamma$ 's approach the observational interval.

Surely, in the case of mixed models, the situation is complicated by the presence of a hot component, which may slow down the gravitational growth in the non-linear regime, in a scale-dependent fashion. Previous results for mixed models concerned a mix including 30 % of HDM, due to a single  $\nu$  with mass  $m_\nu \simeq 7 \text{ eV}$ . Here we deal with  $\nu$ 's 3–4 times lighter; accordingly, when cluster formation begins, their speeds are  $\sim 3$ –4 times greater. Peculiar effects of MDM are therefore significantly reinforced. Hence, besides of having a suitable spectral slope, the mixed models treated here are still more different from standard CDM, because of the late  $\nu$  derelativisation.

In this paper we showed that critical CDM models, with a blue spectrum suitably “compensated” by a light- $\nu$  component, besides of fitting most LSS and CMB data, are able to follow APM and Abell cluster clustering data. This result adds to those discussed in Paper I, where critical blue mixed models were shown to provide a good fit to the cluster mass function and to be in agreement with Donahue et al. (1998) findings concerning high- $z$  cluster abundance.

## REFERENCES

- Abdurashitov J.N. et al., 1996, Phys. Rev. Lett. 77, 4708
- Achilli S., Occhionero F., & Scaramella R., 1985, ApJ, 299, 577
- Athanassopoulos et al., 1995 Phys. Rev. Lett., 75, 2650
- Bahcall N. & Burgett W.S., 1986, ApJ, 300, L35
- Bahcall N. & Cen R., 1992, ApJ, 398, L81
- Bahcall N.A., & Soneira R.M., 1983, ApJ, 270, 20
- Bahcall N.A., & West M.J., 1992, ApJ, 393, 419
- arger V., Weiler T.J., Whisnant K., 1988, PL B, 427, 97
- Baugh C.M., & Gatzagaña E., 1996, MNRAS, 280, L37
- Bonometto S.A., & Pierpaoli E., 1998, NewA 3, 391
- Bonometto S.A., & Valdarnini R., 1984, Phys. Lett., A103, 369
- Bonometto S.A., & Valdarnini R., 1985, ApJ, 299, L71
- Borgani S., Martinez V.J., Perez M.A., & Valdarnini R., 1994, ApJ, 435, 37
- Bradley, E., 1982, in The Jackknife, the Bootstrap, and Other Resampling Plans, CBMS-NSF Regional Conf. SER., in Appl. Math.
- Colberg J.M., White S.D.M., Jenkins A.R., Pearce F.R., Frenk C.S., Thomas P.A., Hutchings R.M., Couchman H.M.P., Peacock J.A., Efsthathiou G.P., & Nelson A.H., 1997, The Virgo Consortium: The evolution & formation of galaxy clusters, in Large Scale Structure: Proc. of the Ringberg Workshop Sept. 1996, ed. D.Hamilton, preprint astro-ph/970286

- Cole S., Weinberg D.H., Frenk C.S., & Ratra B., 1997, MNRAS, 289, 37
- Couchman H.M.P., 1991, ApJ, 268, L23
- Croft R.A.C., Dalton G.B., Efstathiou G. & Sutherland W.J., 1997, MNRAS, 291, 305
- Croft R.A.C., & Efstathiou G., 1994, MNRAS 267, 390
- Dalton G.B., Efstathiou G., Maddox S.J. & Sutherland W.J., 1992, ApJ, 338, L5
- Davis M., Summers F.J. & Schlegel M., 1992, Nat. 359, 392
- Dekel A., Blumenthal G.R., Primack J.R. & Olivier S., 1989, ApJ 338, L5
- Donahue M., Voit G.M., Gioia I., Luppino G., Hughes J.P., & Stocke J.T., 1998, ApJ, 502,  
550
- Efstathiou G., Davis M., Frenk C.S., & White S.D.M., 1985, ApJS, 57, 241
- Efstathiou G., Bond J.R. & White S.D.M., 1992, MNRAS 258, p1
- Eke V.R., Cole S., & Frenk C.S., 1996, MNRAS, 282, 263
- Fukuda Y. et al., 1994, Phys. Lett. B, 335, 237
- Gardini A., Bonometto S.A. & Murante G., 1999, ApJ, 524, 510
- Ghigna S., Borgani S., Bonometto S.A., Guzzo L., Klypin A., Primack J.R., Giovanelli R.  
& Haynes M., 1994, ApJ, 437, L71
- Governato F., Babul A., Quinn T., Tozzi P., Baugh C.M., Katz N., & Lake G., 1999,  
MNRAS, 307, 949
- Gross M.A.K., Somerville R.S., Primack J.R., Holtzman J., & Klypin A., 1998, MNRAS,  
301, 81

- Hampel W. et al., 1996, *Phys. Lett. B*, 388, 384
- Hauser M.G. & Peebles P.J.E., 1973, *ApJ* 185, 757
- Holtzman J.A., 1989, *ApJS*, 71, 1
- Jing Y.P., Plionis M. & Valdarnini R., 1992, *ApJ* 389, 499
- Kaiser N., *ApJ*, 284, L9
- Klypin A., Borgani S., Holtzman J., & Primack J.R., 1995, *ApJ* 444, 1
- Klypin A., Holtzman J., Primack J. & Regós E., 1993, *ApJ*, 416, 1
- Klypin A. & Kopylov, A. I., 1983, *SVAL*, 9, 41
- Klypin A., Nolthenius R., & Primack J.R., 1997, *ApJ*, 474, 533
- Klypin A. & Rhee G., 1994, *ApJ*, 428, 399
- Lee S., & Park C., 1999, *ApJ*, submitted preprint astro-ph/9909008
- Liddle A.R., Lyth D.H., Viana P.T.P. & White M., 1996, *MNRAS*, 282, 281
- Lucchin F., Colafrancesco S., De Gasperis G., Matarrese S., Mei S., Mollerach S., Moscardini L., & Vittorio N., 1996, *ApJ*, 459, 455
- Nichol R.C., Collins C.A., Guzzo L. & Lumsden S.L., 1992 *MNRAS* 255, 21P
- Peacock J.A., & Dodds S.J., 1994, *MNRAS*, 267, 1020
- Peacock J.A., & Dodds S.J., 1996, *MNRAS*, 280, L19
- Peacock J.A., & West M.J., 1992, *MNRAS*, 259, 494
- Perlmutter S., et al., 1998, *Nature*, 391, 51

- Pierpaoli E., & Bonometto S.A., 1998, MNRAS, 305, 425
- Postman M., Huchra J.P. & Geller M.J., 1992, ApJ 384, 404
- Primack J.R., Holtzman J., Klypin A., & Caldwell D.O., 1995, Phys. Rev. Lett., 74, 2160
- Riess A.G., Nugent P., Filippenko A.V., Kirshner R.P., & Perlmutter S., 1998 ApJ., 504, 935
- Sarkar Uptal 1999, Phys.Rev. D, 59, 31301
- Storrie-Lambardi L.J., McMahon R.G., Irwin M.J., & Hazard C., 1995, High Redshift Lyman Limit & Damped Lyman-Alpha Absorbers, in: Proc. ESO Workshop on QSO A.L., preprint astro-ph/9503089
- Sutherland W.J. & Efstathiou G., 1991, MNRAS 248, 159
- Thomas P.A., Colberg J.M., Couchman H.M.P., Efstathiou G.P., Frenk C.S., Jenkins A.R., Nelson A.H., Hutchings R.M., Peacock J.A., Pearce F.R., & White S.D.M., 1998, MNRAS, 296, 1061
- Valdarnini R., Ghizzardi S., & Bonometto S.A., 1999, NewA, 4, 71
- Walter C. & Klypin A. 1996, ApJ, 462, 13
- Watanabe T., Matsubara T., & Suto Y., 1994, ApJ, 432, 17

Table 1: Parameters of the models; besides of input parameters or quantities derived from the linear theory we report the value of  $N_{cl}$  (sim) (number of clusters of mass  $> 4.2 \times 10^{14} h^{-1} M_{\odot}$  in a box side of  $100 h^{-1} \text{Mpc}$ ) as obtained in Paper I. The normalization to COBE quadrupole was deliberately kept at the  $\sim 3\sigma$  lower limit, in order leave some room to the contribution of tensor modes, but keeping however consistent with data. The expected interval for  $N_{cl}$  is 4–6, but models with  $N_{cl}$  up to 8–10 cannot be safely rejected.  $L_{\alpha} \equiv \Omega_b \Omega_{\text{coll}}(z = 4.25, M = 5 \times 10^9 h^{-1} M_{\odot}) \times 10^3$  accounts for the amount of gas expected in Damped Lyman- $\alpha$  systems. More details can be found in Paper I. Data provided by Storrie-Lombardi et al. (1995) give  $L_{\alpha} > 2.2 \pm 0.6$ . This is one of the most stringent indicators of the model capacity to produce high- $z$  objects.

	MDM1	MDM2	TCDM
$\Omega_h$	0.26	0.14	—
$m_{\nu}/\text{eV}$	3.022	1.627	—
$\Omega_b \cdot 10^2$	6.8	9	6
$n$	1.2	1.05	0.8
$Q_{PS,rms}/\mu\text{K}$	12.1	13	17.4
$\sigma_8$	0.75	0.62	0.61
$\Gamma$	0.18	0.23	0.32
$N_{cl}$ (PS; $\delta_c = 1.69$ )	14.	5.2	5.7
$N_{cl}$ (sim)	10.	4.7	6.0
$L_{\alpha}$	1.3	1.2	1.3

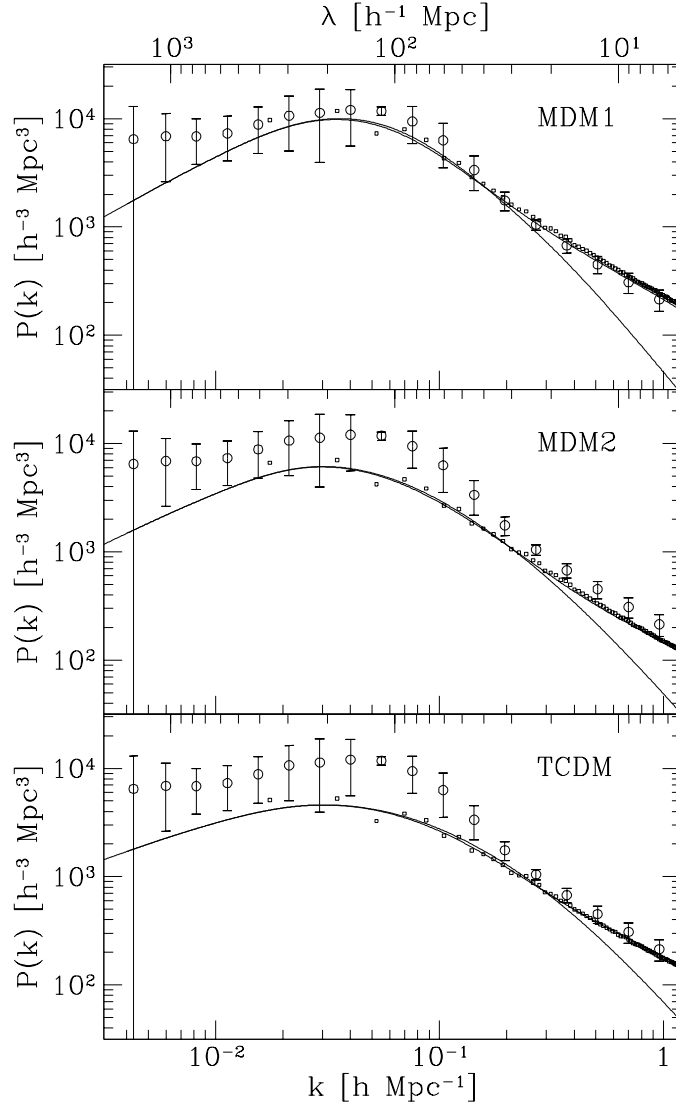


Fig. 1.— Spectra of the three models at  $z = 0$ . Solid curves give the linear power spectrum and the spectrum corrected for non-linearity, according to Peacock & Dodds (1996). Empty squares yield the simulation spectra corrected for CIC (cloud-in-cell; see paper I for more detail). Circles with  $2\sigma$  errorbars are the power spectrum measured from the APM survey.

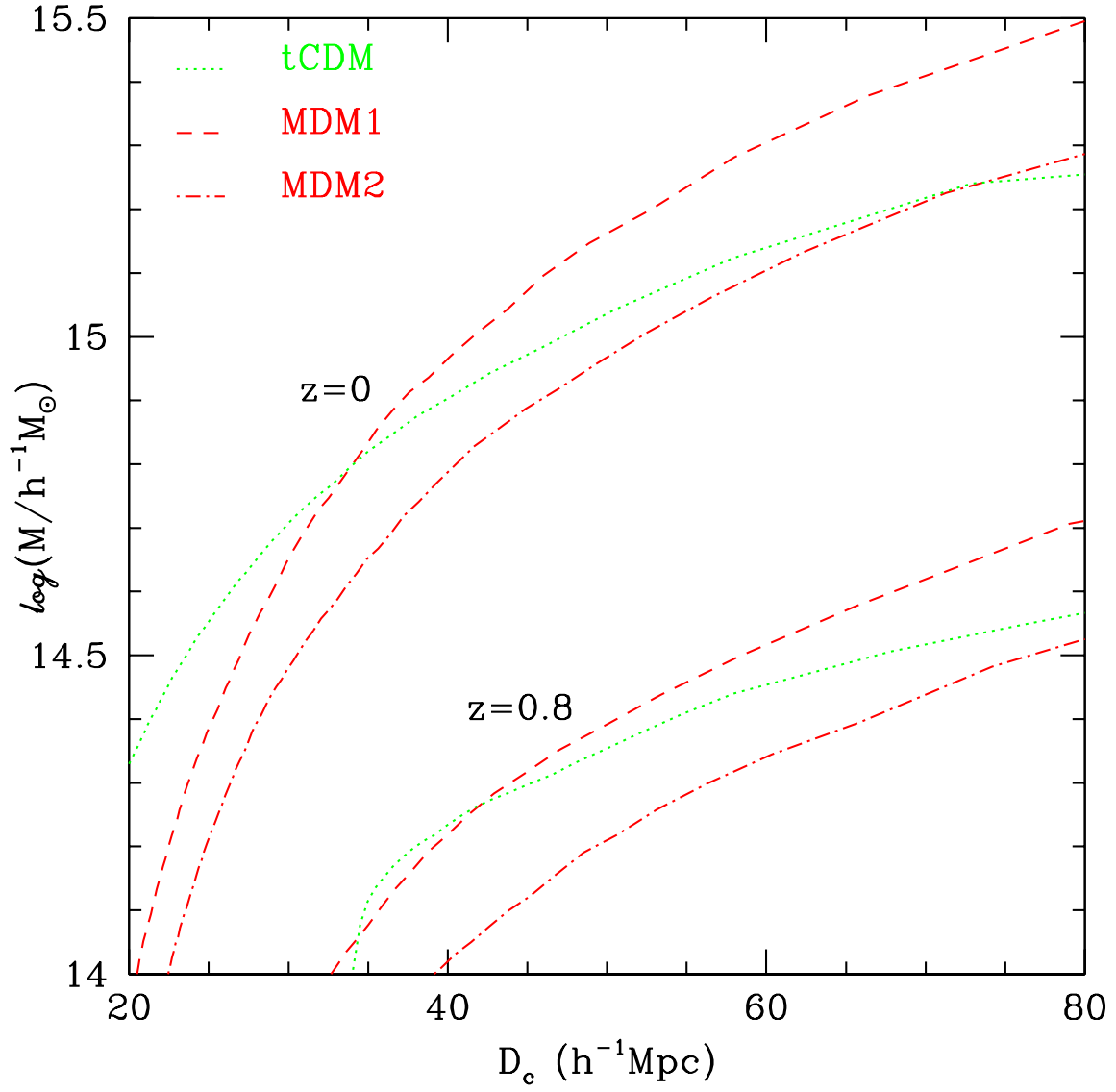


Fig. 2.— Mass limit ( $M_{th}$ ) of cluster samples with mean separation  $D_c = n^{-1/3}( > M_{th})$ .



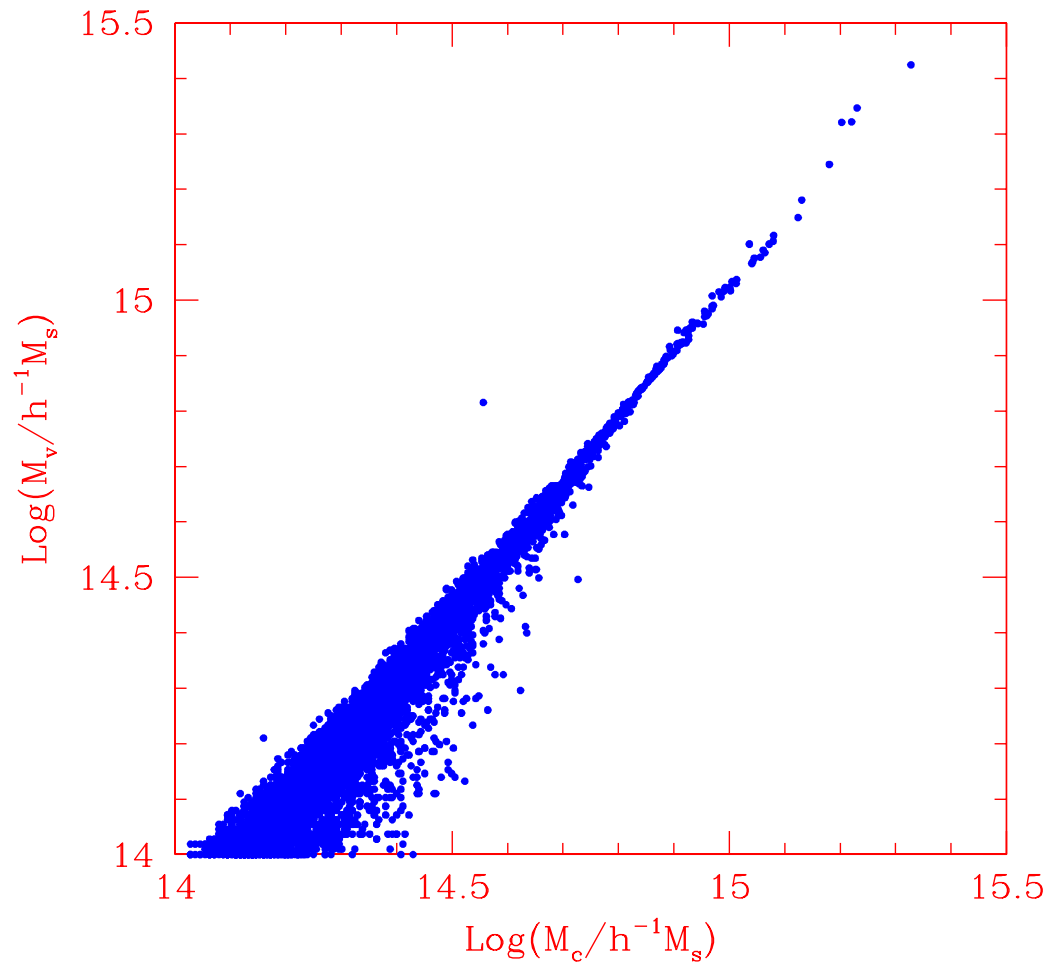


Fig. 3.— All clusters with  $M_c > 10^{14}h^{-1}M_\odot$  are found to contain a virialized halo. Its mass  $M_v$  is shown, as a function of  $M_c$ , for the tCDM model.

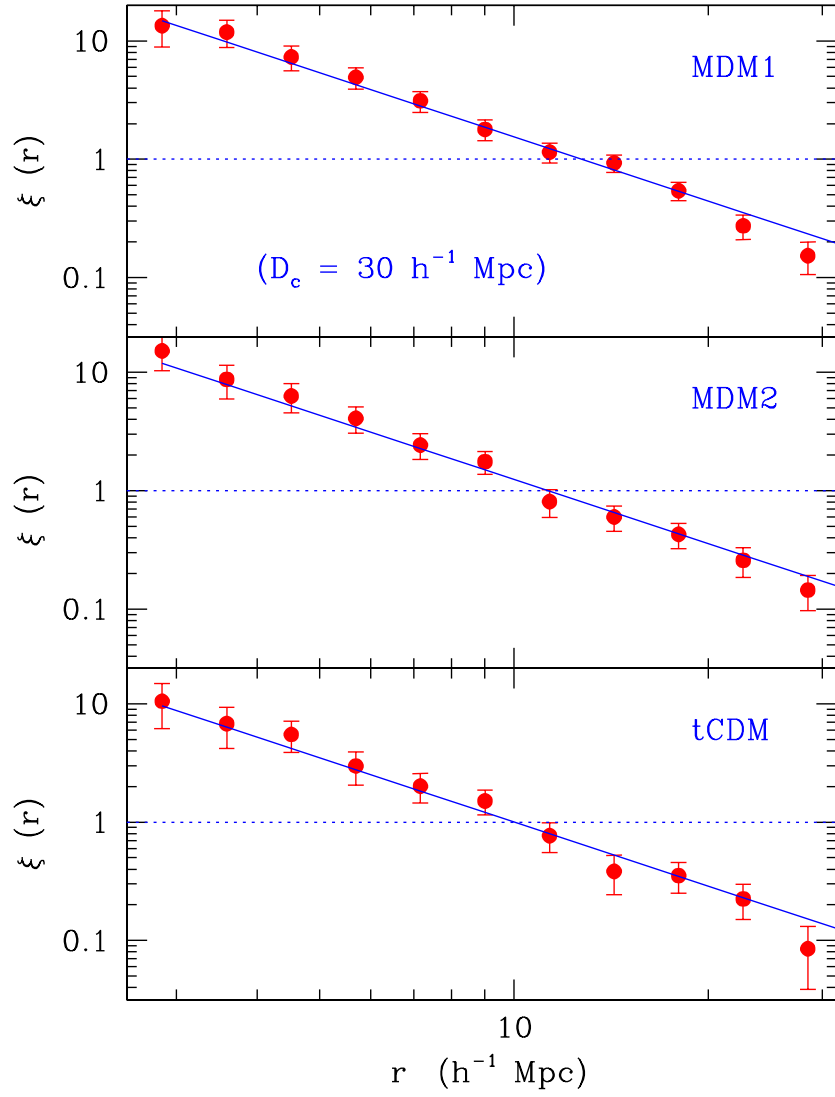


Fig. 4.— The 2–point correlation function estimate (solid points) and  $1\sigma$  bootstrap error bars for  $D_c = 30 h^{-1} \text{ Mpc}$ . A constrained fit with  $\gamma = 1.8$  is also shown (solid line).

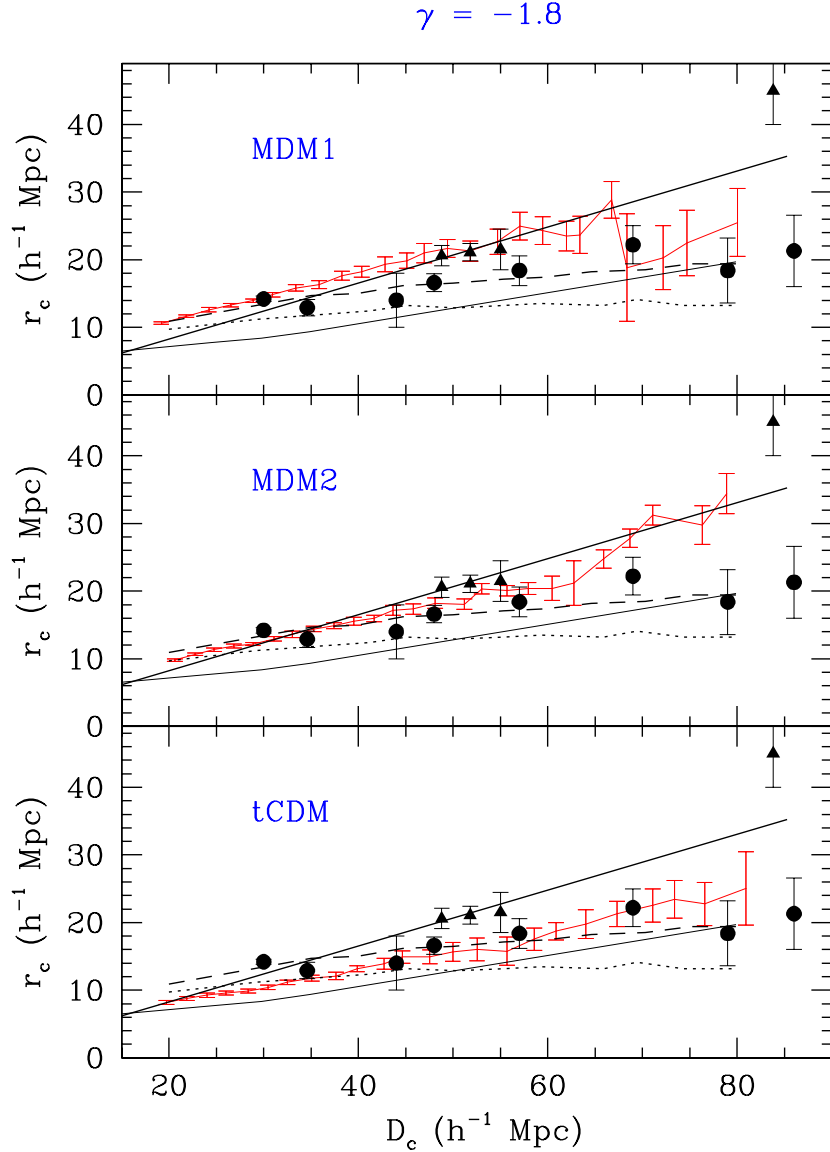


Fig. 5.— The cluster correlation length  $r_c$  as a function of  $D_c$ , for the three models. Here  $r_c$  is obtained by requiring  $\gamma = 1.8$ .  $1\sigma$  bootstrap error bars are also shown.  $r_c$  values obtained from APM and Abell cluster data are also reported (filled circles and triangles, respectively). The thick solid line corresponds to the BW conjecture. Results of SCDM simulation of Bahcall & Cen (1992) are shown by the thin solid line, while dashed and dotted lines refer to Croft et al (1997) simulations of LCMD and SCDM models.

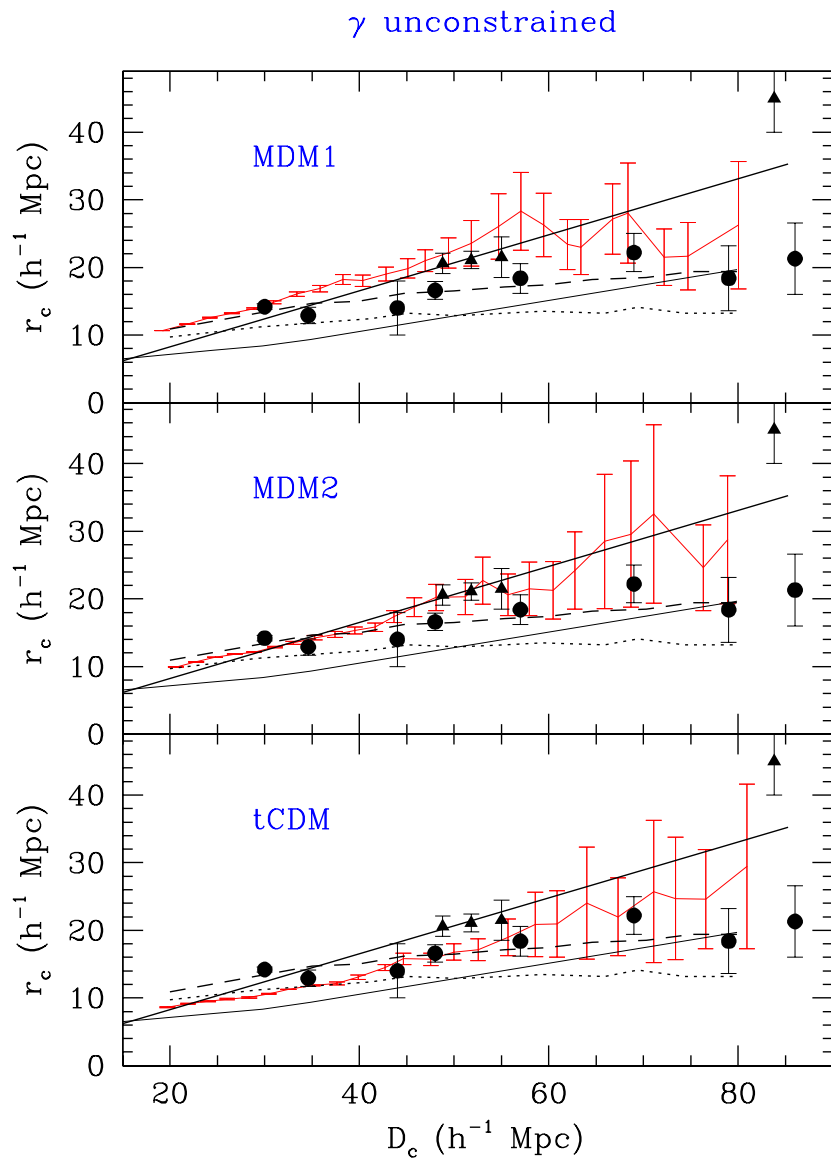


Fig. 6.— Same as Fig 5 but with  $r_c$  obtained by simultaneously fitting it and  $\gamma$  to the halo distribution. Error bars, representing  $1\sigma$  deviation derived from the weighted least-square fits, are obviously larger than in the fixed- $\gamma$  case.

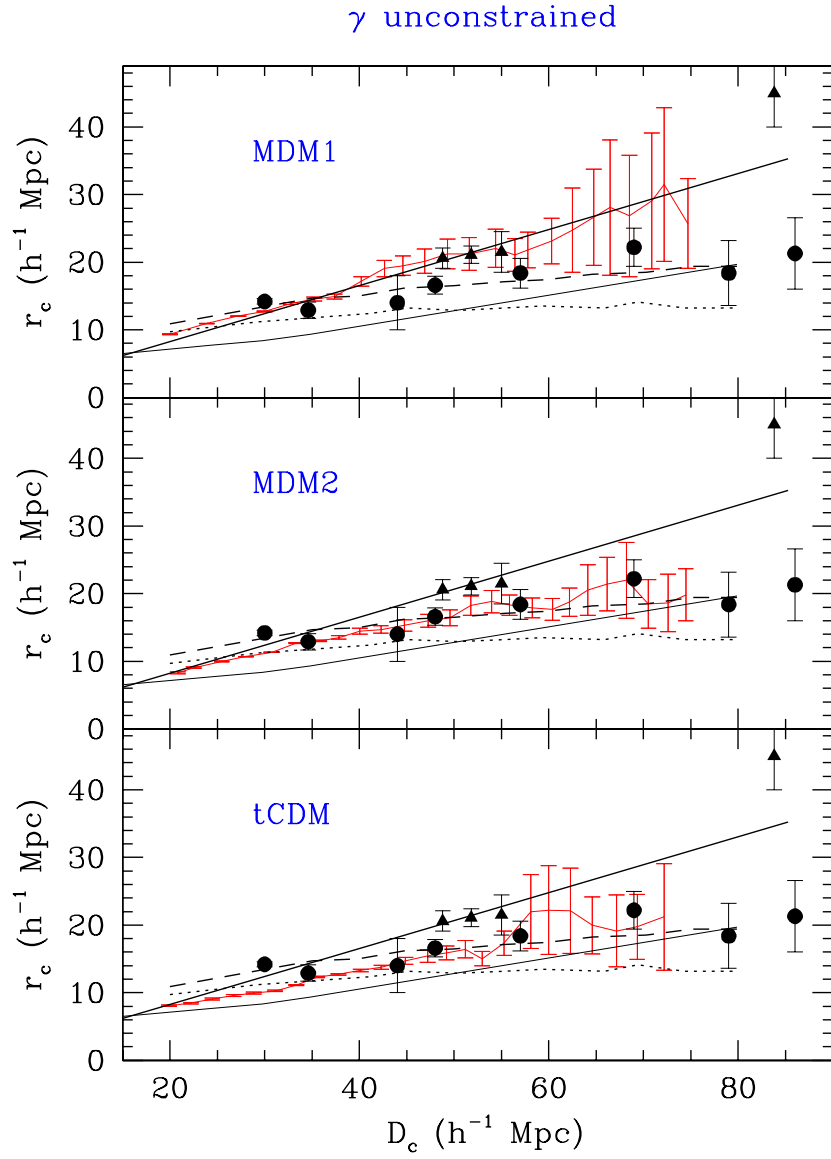


Fig. 7.— Same as Fig 6 but with  $D_c$  obtained ordering clusters according to  $M_v$ .

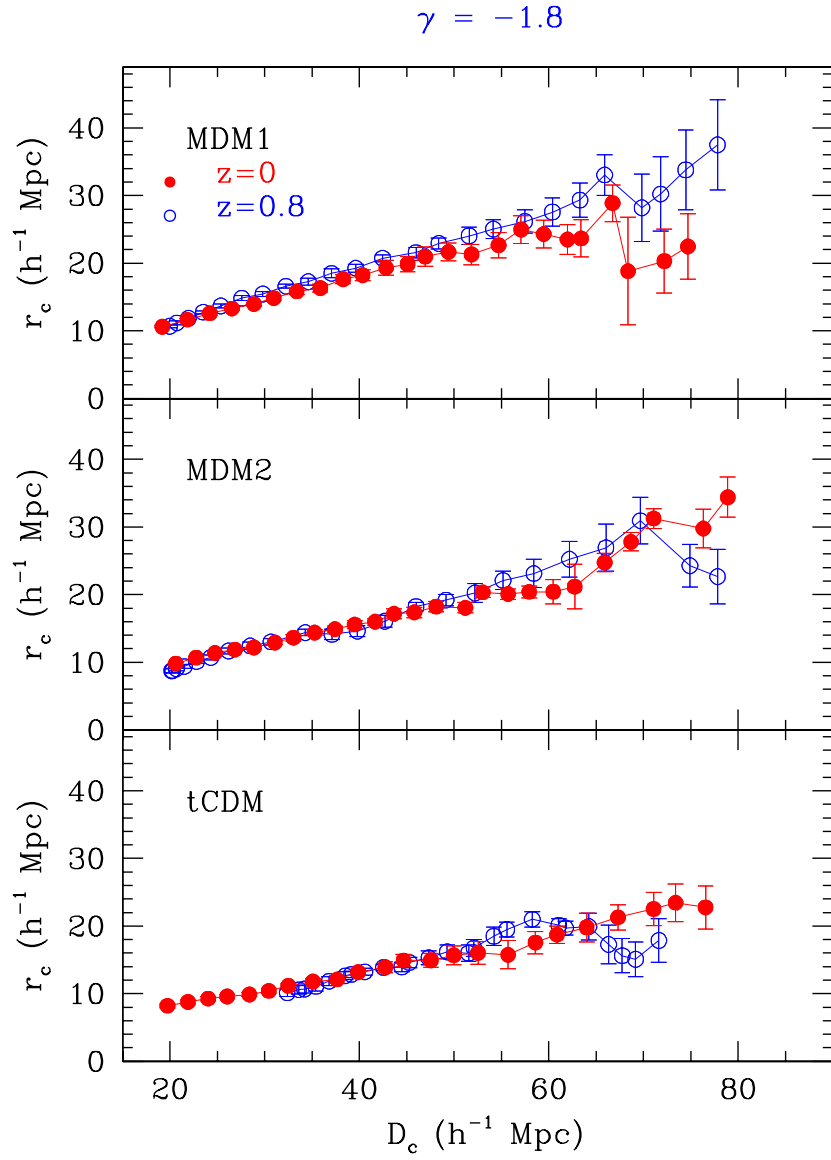


Fig. 8.— Comoving clustering evolution from  $z = 0.8$  to  $z = 0$  obtained by fitting  $r_c$  with  $\gamma = 1.8$ .

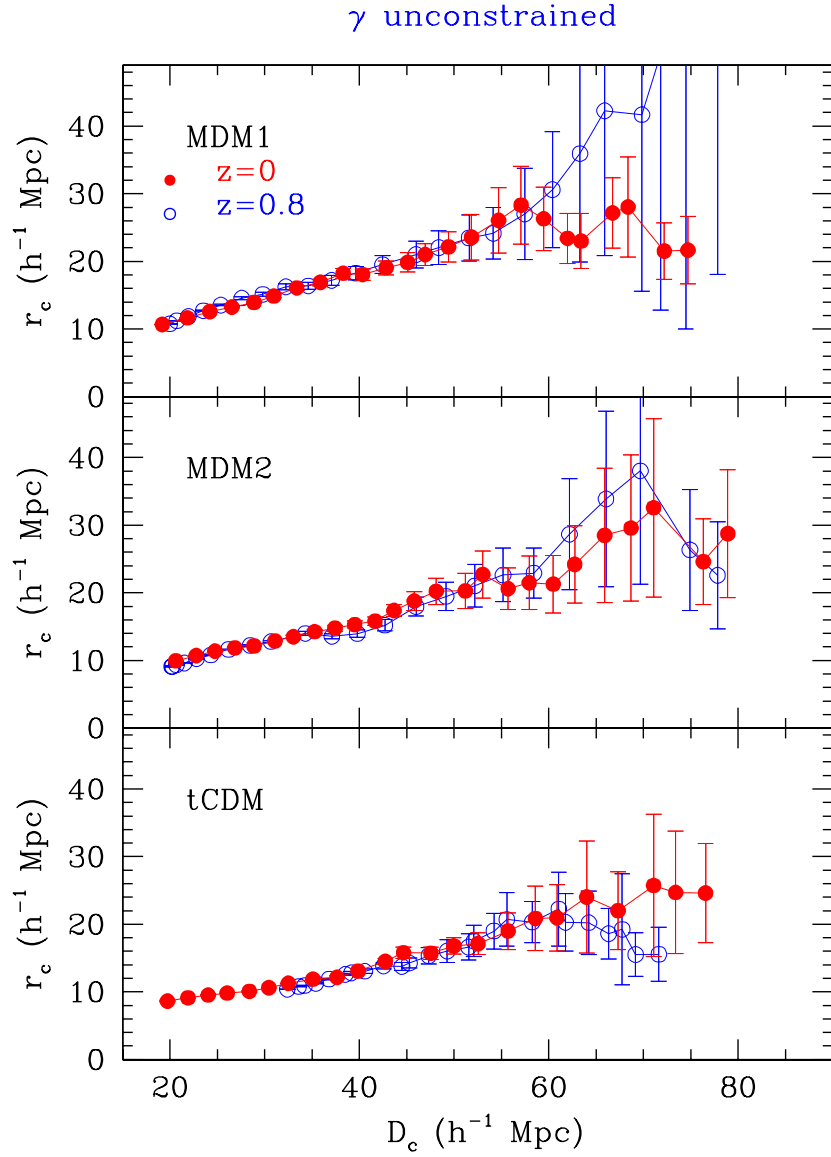


Fig. 9.— Same as Fig 8, but from simultaneous fits of  $r_c$  and  $\gamma$ . MDM1 shows some anomaly.

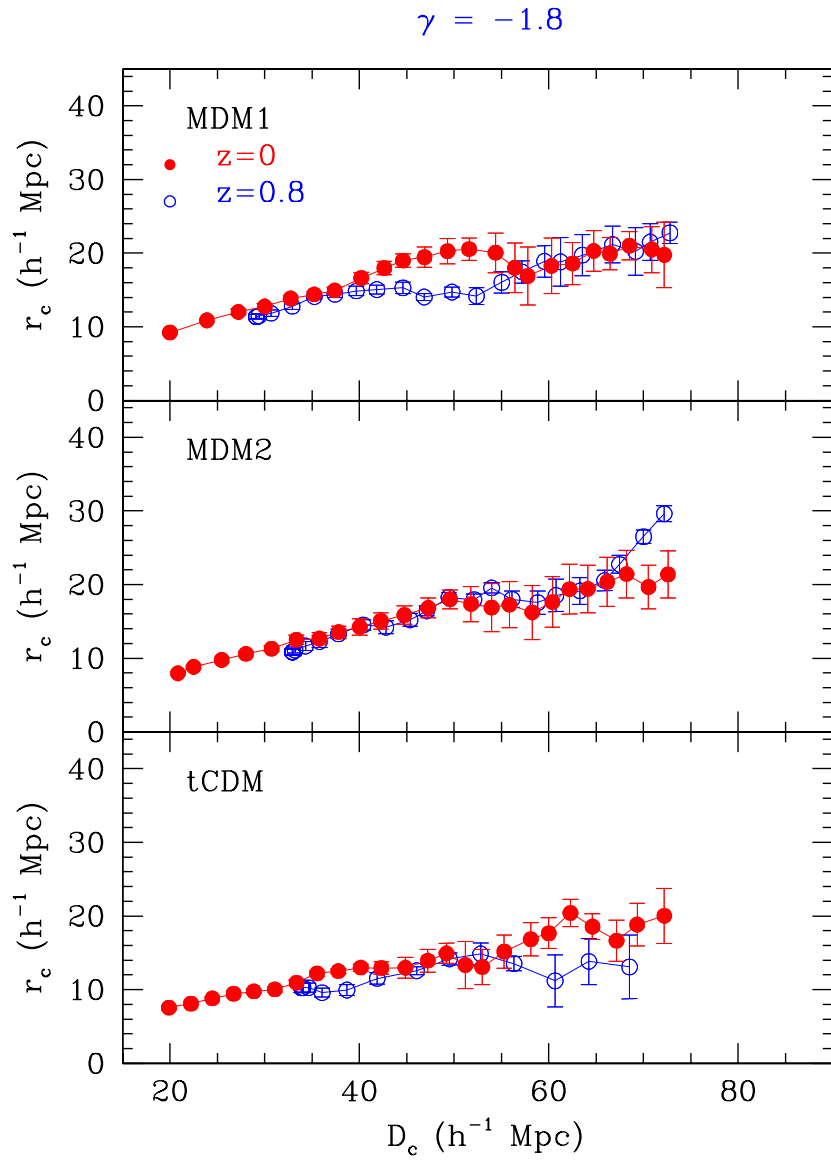


Fig. 10.— The same as Fig 8, but  $D_c$  are obtained ordering clusters according to  $M_v$ . Plots are less noisy, when such mass determination is used.